Demonstration of On-Chip Optical Frequency Comb Generation and Optical Injection Locking

Efstathios Andrianopoulos[1], Nikolaos K. Lyras[1], Tianwen Qian[2], Milan Deumer[2], Georgios Megas[1], Garrit Schwanke[2], Y Durvasa Gupta[2], Panos Groumas[3], Zerihun G. Tegegne[4], Ben Schuler[2], Muhsin Ali[5], Bradley Snyder[4], Simon Nellen[2], Christos Tsokos[1], David de Felipe[2], Maria Massaouti[1], Guillermo Carpintero[5], Robert B. Kohlhaas[2], Joost van Kerkhof[4], Norbert Keil[2], Christos Kouloumentas[3], Hercules Avramopoulos[1]
[1]Photonics Communications Research Laboratory, National Technical University of Athens, Zografou 15573, Athens, Greece
[2]Fraunhofer Institute for Telecommunications, Heinrich-Hertz-Institut, Berlin 10587, Germany
[3]Optagon Photonics, Agia Paraskevi 15341, Athens, Greece
[4]PHIX BV, Enschede 7522, The Netherlands
[5]Universidad Carlos III de Madrid, Madrid 28911, Spain
efand@mail.ntua.gr

Abstract: We experimentally demonstrate for the first time a photonic integrated circuit comprising an optical frequency comb generation unit and an optical injection locking unit, as part of a fully packaged photonic wireless sub-THz receiver module. © 2024 The Author(s)

1. Introduction

Optical injection locking (OIL) is the process in which the light of a primary laser is injected into the cavity of a secondary laser, forcing the latter to synchronize in terms of phase and frequency [1]. As a process, OIL finds use in a plethora of different applications where laser synchronization is necessary. Some indicative examples include local oscillator (LO) generation in homodyne receivers [2], optical atomic clocks [3], optical signal processing [4], and a number of different other applications described in detail by the authors in [1]. Furthermore, due to its inherent ability to generate microwave tones of high purity, OIL has emerged as a key tool in microwave photonics enabled applications for the generation of mmWave and sub-THz wireless signals in optical heterodyning schemes, where phase-locked optical carriers are either used at the transmitter side, to down-convert the modulated signal from the optical domain to the microwave domain, or at the receiver side, to create a stable photonic LO in photoconductive antenna (PCA) based applications [5]-[7].

On a related note, photonic integrated circuits (PICs) have emerged as a transformative advancement in optical technologies, offering a spectrum of compelling advantages. Among those, their inherent miniaturized nature enables substantial size and weight reduction, enabling the consolidation of multiple optical functionalities in a single microchip. To add on that, the rise of hybrid photonic integration enables the combination of the strengths of various photonic technologies and platforms, allowing for the incorporation of both passive and active optical elements to create powerful and versatile integrated optical engines.

In this work we present a fully packaged PIC-based module whose functionality is that of a wireless sub-THz photonic receiver, comprising different operations i.e., optical frequency comb generation (OFCG), OIL, optical down-conversion, wireless detection, and amplification. To our specific interest in this work, the module's OFCG and OIL units are evaluated. To the best of our knowledge, this is the first experimental demonstration of a fully packaged PIC encompassing OFCG as well as OIL functionalities enabled by an integrated isolator between them, whose field of application can be expanded in a plethora of different optical technologies.

2. Photonic integrated circuit (PIC) presentation

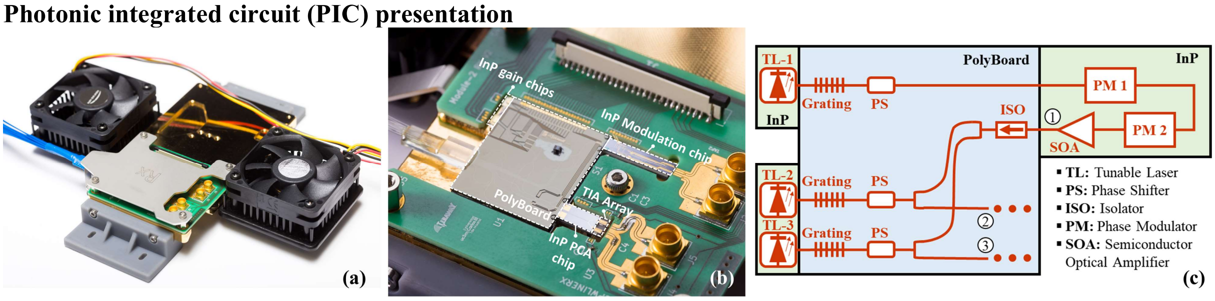

Figure 1: (a) Picture of the packaged TERAWAY module, (b) Picture of the module's PIC, and (c) Functional schematic of the module's evaluated operations in this work

Figure 1 demonstrates the PIC under discussion in this work. A picture of the fully packaged optical engine is shown in Figure 1a. The PIC of the module is placed beneath a metal lid used to protect it from both dust contamination and potential damage due to direct contact. A fiber array is accommodated, enabling the calibration and configuration of the individual optoelectronics building blocks. Its electrical configuration is realized through a printed circuit board (PCB) which is connected to the PIC via DC and RF wirebonds. The PCB hosts SMP and FFC/FPC connectors to facilitate the interconnection of the PIC with commercially available test and measurement equipment. From the thermal management point of view, the module encompasses a Peltier thermoelectric cooler (TEC), two forced convection heat sinks equipped with fans, and a heat spreader (heat pipe). The module is placed on a Cu plate to ensure thermal dissipation through the fan drive heatsinks.

A close-up picture of the PIC is depicted in Figure 1b. The PIC consists of the hybrid integration of four individual photonic chips from different technology platforms, exhibiting complementary functionalities. Firstly, an InP chip encompassing three gain sections offers the optical sources of the PIC (upper-left side of the PIC). A polymer-based hybrid photonic integration platform named PolyBoard [8] serves as the photonic motherboard of the PIC, incorporating the tunable distributed Bragg reflector (DBR) lasers' external cavities, the routing network, optical couplers, an optical isolator [9], as well as 90-10 tap couplers to be used for monitoring purposes (center of the PIC). An InP chip enables the PIC's modulation stage consisting of two cascaded phase modulators (PMs) and a semiconductor optical amplifier (SOA, upper-right side of the PIC). Finally, the PIC comprises an InP chip consisting of PCAs integrated with an on-chip transimpedance amplifier (TIA) array (lower-right side of the PIC).

To our specific interest in this work, the OFCG and optical injection locking operations are evaluated, the schematic of whom is depicted in Figure 1c. A DBR tunable laser (TL-1) acts as the primary laser, and serves as the input at the OFCG stage, consisting of two cascaded PMs and an SOA. When driven with sinusoidal waves, the PMs generate multiple optical tones at distances defined by the frequency of the sine wave, yielding a comb resembling optical spectrum, called an optical frequency comb (OFC). An isolator whose output is equally split in two paths is responsible for injecting the OFC in the secondary DBR lasers (TL-2 and -3). The tunability of the DBRs is performed by applying current to their cavities' grating and phase section, providing a 20 nm tuning range [8]. Thus, phase-locking is achieved by carefully tuning the output wavelengths of the two secondary DBRs to coincide with the desired tones of the OFC. Monitoring of the spectra of the OFC, as well as of the two secondary DBRs is enabled by the fiber array described earlier.

3. Experimental results and discussion

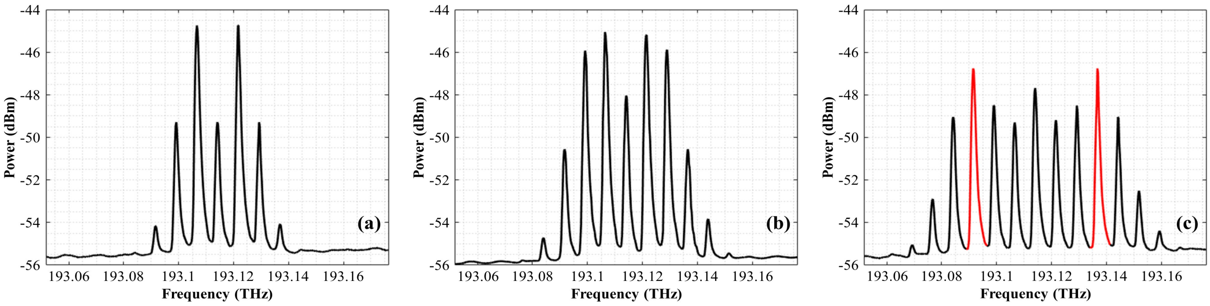

Figure 2: Spectra of the generated OFCs: (a) PM1 individually, (b) PM2 individually and (c) PM1 & PM2 combined

The experimental evaluation we followed was two-fold. In the first step, we assessed the performance of the OFCG, monitoring the spectrum directly after the SOA at point (1) denoted in Figure 1c, using the corresponding fiber array port. To that end, an RF LO was used, providing sinusoidal waves at the RF inputs of the PMs through the SMP connectors hosted at the module's PCB. The performance evaluation was firstly realized for each PM individually, followed by the evaluation of the PM cascade. In the latter scenario, the output of the LO was equally split into two electrical paths, with an RF phase shifter accommodated in one of them to control the relative phase shift of the sinusoidal waves driving the PMs. In each case, equal power was fed into the corresponding SMP connector of each PM (20 dBm). The results of this evaluation are presented in Figure 2. More specifically, Figure 2a, b depict the OFCs obtained from PM1 and PM2 respectively. As can be observed, PM2 exhibited a better performance than PM1 when driven with the same RF power, generating seven optical tones with adequate optical power compared to PM1 which generated five. Considering that the PMs have identical design, any $V\pi$ variations between the two are expected to be negligible, and thus this mismatch is most likely attributed to lower RF power reaching PM1 [10]. When driven concurrently, the PM cascade yields a broad OFC, shown in Figure 2c, where the 3rd order harmonics (denoted with the red color) are maximized, symmetrically of the optical carrier. Taking into account the resolution of the available optical spectrum analyzer (OSA) which was equal to 0.02 nm (~2.5 GHz in C-band), and the electrical bandwidth of our electrical spectrum analyzer (ESA), equal to 50 GHz, the frequency of the RF LO which

provided the best trade-off between these two factors was 7.5 GHz, allowing us to perform the injection locking process with the 3rd order harmonics, whilst being able to clearly assess the shape of the OFC.
At the second step, we examined the performance of the generated microwave tone. To do that, we firstly tuned the output wavelengths of the two secondary lasers to coincide with the 3rd order harmonics of the comb, monitoring their spectra in free-running mode (without OFC injection) at points (2) and (3) denoted in Figure 1c. Considering that the frequency of the LO was equal to 7.5 GHz, these harmonics had a frequency distance of 6x7.5 GHz equal to 45 GHz. Then, we injected the OFC into the DBRs performing the phase-locking process and, using an on-chip Mach-Zehnder interferometer, we forwarded one output to an external photodetector (PD), feeding its output to our ESA, whereas the other was used for monitoring purposes, feeding the optical signal into our OSA. Since the fiber array monitoring ports are fed by the 10% tap couplers, an external erbium-doped fiber amplifier was used to provide adequate power to the PD. The generated microwave tone is depicted in Figure 3. The central frequency of the microwave tone was equal to 45 GHz in all scenarios, defined by the frequency of the LO. Figure 3a depicts the electrical spectrum of the generated microwave tone, when the two DBRs operate in a free-running mode. As observed, the tone exhibits frequency instabilities due to the lasers' uncorrelated phase noises, leading to wider spectral content around its central frequency. As shown in Figure 3b and c, depicting the locked microwave tone, through the injection locking process the phase noises of the two secondary DBRs become correlated and are therefore suppressed during the photodetection stage. The generated microwave tone has almost negligible phase noise, with a 3-dB linewidth below the resolution of the ESA, which was set at 100 Hz.

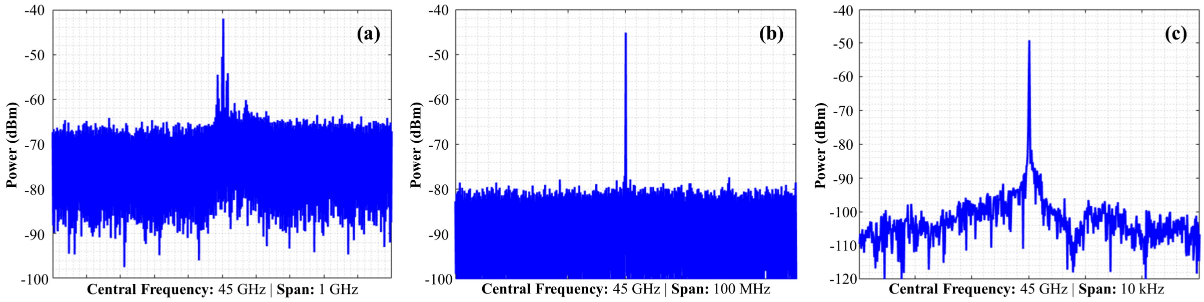

Figure 3: Spectra of the microwave tone after photodetection. (a) Unlocked tone, Span: 1 GHz (b) Locked tone, Span: 100 MHz (c) Locked tone, Span: 10 kHz

Extension to higher frequencies seems straight-forward, considering that the effectiveness of the injection locking process is predominantly defined from the injected power and that the power of each harmonic of an OFC is not dependent on the frequency of the RF sinusoidal wave, but rather on the ratio of its power to the modulator's $V\pi$ [10]. Therefore, higher LO frequencies could be used leading to generated microwave tones of also higher frequencies, assuming that corresponding test and measurement equipment is available. Optical phase-locking in optical heterodyne communications as a means of tackling the phase noise impairments has been under the under the microscope of the research community, implemented also as a way to generate stable photonic LOs to be fed in PCAs [7]. As a next step, we intend to explore that possibility using the module described in this manuscript, exploiting the PIC's full potential.

4. Acknowledgments

The presented work has been carried out within the framework of the EU-funded Horizon 2020 Research and Innovation Programme TERAWAY [11] (G.A. ID 871668).

5. References

[1] Z. Liu and R. Slavík, "Optical Injection Locking: From Principle to Applications," in JLT, vol. 38, no. 1, pp. 43-59, 1 Jan.1, 2020
[2] Keisuke Kasai et al., "80 Gbit/s, 256 QAM coherent transmission over 150 km with an injection-locked homodyne receiver," Opt. Express 23, 29174-29183 (2015)
[3] Loh, W., Stuart, J., Reens, D. et al. Operation of an optical atomic clock with a Brillouin laser subsystem. Nature 588, 244–249 (2020).
[4] Koichi Hasebe and Fumio Koyama 2006 Jpn. J. Appl. Phys. 45 6697
[5] T. Nagatsuma et al., "300-GHz-band wireless transmission at 50 Gbit/s over 100 meters," 2016 41st IRMMW-THz, 2016, pp. 1-2
[6] A. Morales et al., "Highly Tunable Heterodyne Sub-THz Wireless Link Entirely Based on Optoelectronics," in IEEE Transactions on Terahertz Science and Technology, vol. 11, no. 3, pp. 261-268, May 2021, doi: 10.1109/TTHZ.2021.3064188.
[7] E. Andrianopoulos et al., "Real-Time Sub-THz Link Enabled Purely by Optoelectronics: 90–310 GHz Seamless Operation," in IEEE PTL, vol. 35, no. 5, pp. 237-240, 1 March1, 2023, doi: 10.1109/LPT.2023.3235932.
[8] Felipe et al. "Recent Developments in Polymer-Based Photonic Components for Disruptive Capacity Upgrade in Data Centers" JLT (2017).
[9] Conradi et al., "High Isolation Optical Isolator: A new Building Block for PolyBoard Photonic Integrated Circuits," in ECOC (2018)
[10] V. J. Urick, K. J. Williams, and J. D. McKinney. "Fundamentals of microwave photonics." John Wiley & Sons, 2015.
[11] https://ict-teraway.eu/